

1992

Performance Evaluation of Small Centrifugal Compressors for Application in Air-Cycle Power and Refrigeration System

M. M. Rahman

Mainstream Engineering Corporation

R. P. Scaringe

Mainstream Engineering Corporation

Follow this and additional works at: <https://docs.lib.purdue.edu/icec>

Rahman, M. M. and Scaringe, R. P., "Performance Evaluation of Small Centrifugal Compressors for Application in Air-Cycle Power and Refrigeration System" (1992). *International Compressor Engineering Conference*. Paper 819.
<https://docs.lib.purdue.edu/icec/819>

This document has been made available through Purdue e-Pubs, a service of the Purdue University Libraries. Please contact epubs@purdue.edu for additional information.

Complete proceedings may be acquired in print and on CD-ROM directly from the Ray W. Herrick Laboratories at <https://engineering.purdue.edu/Herrick/Events/orderlit.html>

PERFORMANCE EVALUATION OF SMALL CENTRIFUGAL COMPRESSORS FOR APPLICATION IN AIR-CYCLE POWER AND REFRIGERATION SYSTEMS

by

M.M. Rahman and R.P. Scaringe
Thermal Systems Division
Mainstream Engineering Corporation
200 Yellow Place
Rockledge, Florida 32955

ABSTRACT

The paper presents some experimental and theoretical results of the performance of small centrifugal compressors as a part of ongoing research efforts for the development of small compressors for lightweight power and refrigeration systems. A test facility was developed for the performance evaluation of compressors of different size and blade profile and measurements were performed for two compressors. Dimensional analysis was used to correlate the test data. It was found that with the increase of blade Mach number, the ratios of stagnation pressure and temperature increased monotonically for any given flow condition. For compressors of different size, the Reynolds number was found to be a single function of dimensionless flow coefficient. The test results were supplemented with the results of numerical simulation of flow in impeller blade passages. Detailed three-dimensional flow structure was predicted by solving the equations for the conservation of mass and momentum. As expected, the local fluid velocity in impeller blade passage was found to increase with the rotational speed of the compressor.

INTRODUCTION

Air-Cycle power and refrigeration systems have been traditionally used in industrial gas turbines and for aircraft propulsion and air-conditioning systems. Such systems are usually large and use axial flow turbines and compressors. Centrifugal compressors and radial flow turbines are used in smaller systems like an automotive turbocharger. Both centrifugal and axial flow machines may need a number of stages to get adequate pressure rise for any given operation. For a small flow rate and large pressure rise application like in a vapor compression refrigeration system, positive displacement machines like a reciprocating compressor or a sliding vane rotary compressor need to be used. The present study for the development of small centrifugal compressors was primarily motivated from the efforts of designing a micro-climate cooling system for individual soldiers [1] and a lightweight pollution-free personnel heater for Army tracked vehicles [2]. In addition to the required heating or cooling, these systems needed to be capable of producing electric power for the operation of communication equipment in the

warfield environment. One critical feature in the design of these systems is the minimization of system size and total weight. The use of Brayton cycle [3] for the power and refrigeration loop along with the use of a centrifugal compressor and an axial flow turbine appears to provide the most competitive design for these applications.

The air-cycle microclimate cooling system is schematically shown in Figure 1. A gas turbine using an open-loop Brayton cycle is the prime mover for the system. Atmospheric air is drawn in through the compressor, compressed to a high pressure, and passed to a combustion chamber where a liquid fuel (diesel) is burned at constant pressure. The product of combustion passes through the turbine where mechanical energy is produced to drive the compressor and generator. The generator is also equipped to work as a motor to start the operation of the compressor. The operating conditions for the gas turbine are shown as 1-2-3-4 in P-h and T-s diagrams in Figure 1. The corresponding ideal isentropic conditions for compression and expansion are shown as dashed lines. For the cooling purpose, the compressed air is bled out of the system and passed through a heat exchanger to cool it down by convection to a temperature close to the atmospheric condition. The air coming out of the heat exchanger is passed through a turbine to generate more mechanical energy for the system and expand it to the required temperature. Figure 1 shows this expansion process as 5-6. The dashed line again shows an ideal isentropic expansion. In order to control the humidity of the supply air, the temperature T_d at the exit of the expander is maintained at the required dew point temperature of the supply air. Due to the temperature drop in the heat exchanger and expander, condensation of moisture may take place if the temperature falls below the saturation temperature corresponding to the partial pressure of the water vapor contained in the air. This moisture is removed in the water separator immediately following the expander. A heat exchanger is used to increase the temperature of the supply air from the dew point to the required dry bulb temperature. This process is shown as 6-7 in P-h and T-s diagrams in Figure 1. The fuel in the combustion chamber is supplied by a fuel pump, and the cooling or heating in the above heat exchangers is accomplished by blowing atmospheric air with the help of a blower. Also, the exhaust coming out of the turbine is mixed with atmospheric air in a heat exchanger to discharge it at a safe level of temperature. The three heat exchangers mentioned above are connected in series to operate with a single blower. Atmospheric air first passes through the heat exchanger which follows the water separator, then flows through the heat exchanger before the turbine and is finally mixed with the exhaust in a direct contact heat exchanger. This arrangement provides a large effectiveness since the fluid which is cooled in the first heat exchanger is used as the heat removal medium in the second heat exchanger.

The optimum operating conditions for any given temperature and humidity conditions of the ambient atmosphere can be determined from the thermodynamic analysis of the cycle as presented by Rahman and Scaringe [1]. Since the compressor is the key component in the operation of the power and cooling loops and the overall system efficiency depends on the performance of the compressor, the present study is undertaken to understand more details about the operation of this component. Both experimental measurements and theoretical calculations were performed to understand the energy transfer process and flow structure in small compressors that can be potentially used in air-cycle power and refrigeration system. Since the present work is a part of ongoing research efforts, it is expected that the results presented here may be significantly improved in future presentations, as more experimental data and numerically predicted results become available and a lightweight centrifugal compressor is developed based on thermal, structural and material considerations.

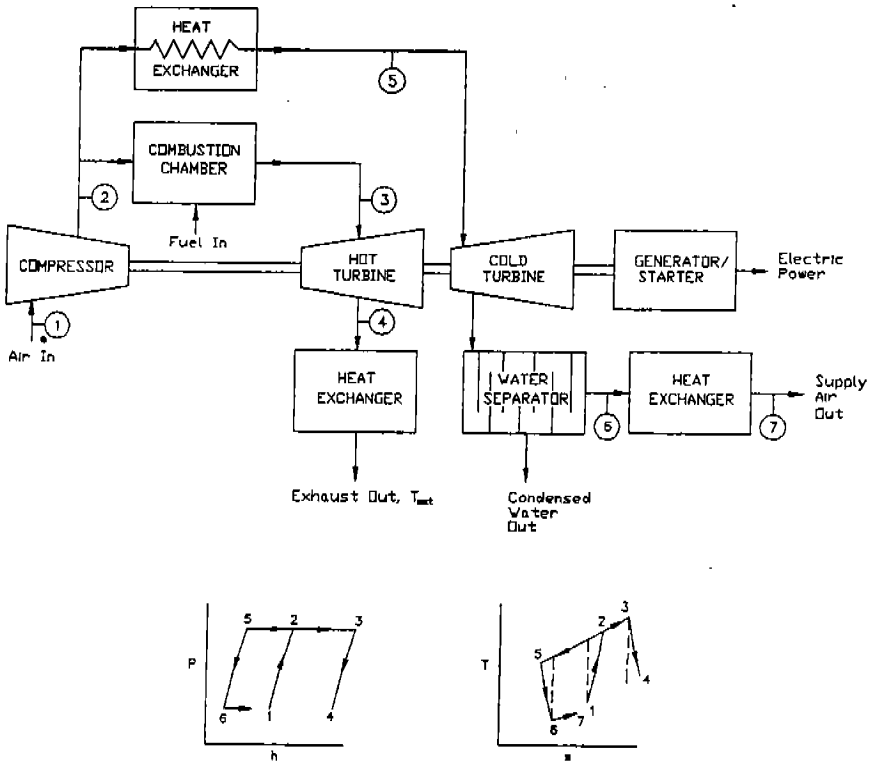


Figure 1. Schematic of the Air-Cycle Microclimate Cooling Device

EXPERIMENTAL MEASUREMENTS

The test facility used for the experimental measurements of the flow in centrifugal compressors is schematically shown in Figure 2. The measurements included the speed of rotation, flow rate, and pressure and temperature at the inlet and exit of the compressor. The compressor was driven by a variable speed electric motor. The RPM of the motor was measured by a tachometer. Air was drawn in through a converging bell mouth section to have a well-ordered flow at the entrance to the flow meter. The flow rate was controlled by a ball valve located at the exit end of the system. The flow rate was measured with a differential pressure flowmeter installed at the entrance line to the compressor. The calibrated range of this meter was 0-400 SCFM. Due to limited accuracy of the visual readout of this meter, an additional device was used to cross-check the flow rates. The primary differential pressure drop across the flow meter sensor was read out using a differential pressure transducer of the range of 0-15 in H₂O, and the flow rate was calculated using an equation supplied by the manufacturer. This latter method yielded a very accurate determination of flow rate, particularly at low flow runs.

Pressure and temperature sensors were placed close to the entrance and exit to the compressor to avoid losses in the plumbing. For the measurement of pressure, two Setra pressure transducers were used. The absolute pressure at the entrance to the compressor was measured with a transducer of the range of 0-25 psia. The difference between inlet and exit pressures was measured using a differential pressure transducer of the range 0-5 lb/in². The measurement of pressure difference instead of absolute pressure for the exit was done to get a more accurate determination of pressure since pressure rise was not very high, particularly at large flow rates. Two Gordon 4-wire RTDs were used to measure inlet and exit temperatures.

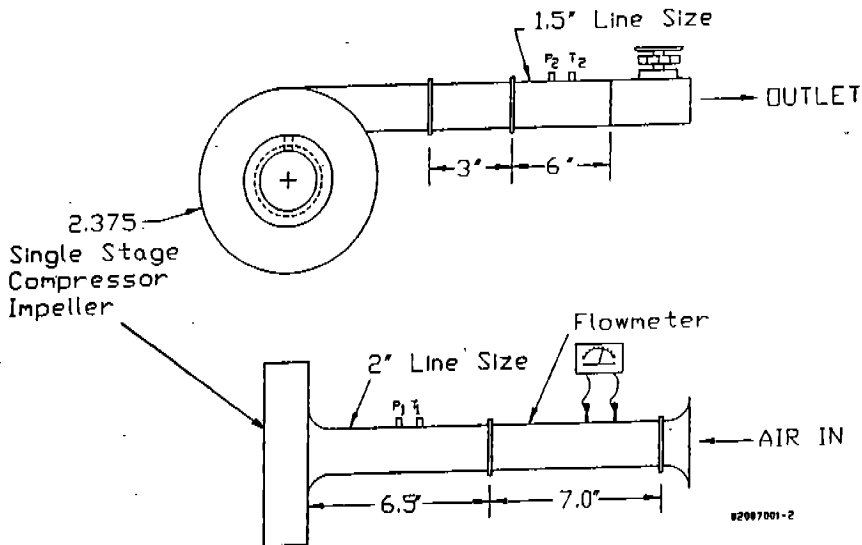


Figure 2. Experimental Test Facility

Experimental measurements were performed for two compressors with different impeller sizes. The diameter and height of the impeller for the smaller compressor was 2.365 and 0.773 inches, respectively. The larger compressor had a diameter of 2.48 inch and height of 0.91 inch. This provided a height to diameter ratio (H/D) of 0.33 and 0.37, respectively. The impellers had very similar blade profiles. The measurements of pressure, temperature, flow, and speed were performed simultaneously and were automatically recorded using a Fluke Hydra Datalogger. The speed of rotation of the motor was controlled by adjusting the frequency of the power supply, and the flow rate was controlled by controlling the opening of the valve. The measurement of data was started before starting the motor to record the ambient conditions and any offset in the measuring devices. Then the motor was started and gradually adjusted to the required speed. Scanning of data was done every 30 seconds and was recorded when temperature readings approached a steady-state condition. The pressure and flow readings reached steady state condition fairly quickly, but temperature adjustment appeared to persist over a period of 3 to 15 minutes. The data were checked for consistency in terms of pressure and temperature rise. The repeatability of the test results was also investigated for both compressors by repeating certain runs and comparing the results. It was found that the test results were repeatable within a small tolerance.

The experimental data were used to calculate the mass flow rate, pressure ratio, and different dimensionless parameters identified from dimensional analysis [4-5]. The parameters that are significant for the flow in a centrifugal compressor are:

$$\text{Flow coefficient} = m(R T_{01})^{1/2}/(D^2 P_{01})$$

$$\text{Blade Mach number} = N D/(\gamma R T_{01})^{1/2}$$

$$\text{Reynolds number} = m/(\mu D)$$

$$\text{Stagnation pressure ratio} = P_{02}/P_{01}$$

$$\text{Stagnation temperature ratio} = T_{02}/T_{01}$$

$$\text{Height to diameter ratio} = H/D$$

where

D	=	Diameter of the impeller (m)
H	=	Height of the impeller (m)
N	=	Rotational speed (rev/s)
m	=	Mass flow rate (Kg/s)
P ₀₁	=	Stagnation pressure at inlet (Pa)
P ₀₂	=	Stagnation pressure at outlet (Pa)
T ₀₁	=	Stagnation temperature at inlet (K)
T ₀₂	=	Stagnation temperature at outlet (K)
R	=	Gas constant (J/Kg K)
γ	=	Ratio of specific heat
μ	=	Viscosity (N.S/m ²)

The variation of outlet to inlet static pressure ratio with blade Mach number is presented in Figure 3. It can be seen that, for both impellers, the pressure ratio increases with Mach number. The range of Mach number variation in the present experiment is between 0.2 and 0.5. At this condition, the effect of compressibility is expected to be relatively small and the flow may not encounter any choking. The rise of static pressure is small, to a maximum of 4 percent, for the rotational speed used in the present experiment. With the increase of rotational speed, the blade Mach number increases, which consequently increases the pressure ratio. It can also be seen that the rise of pressure ratio with blade Mach number is almost monotonic for a given valve setting, which controls the flow coefficient. The flow coefficient and Mach number are two independent parameters for the flow in a compressor.

Figure 4 shows the distribution of stagnation pressure ratio as a function of blade Mach number. The stagnation pressure also increases monotonically with Mach number for a given flow coefficient. It can be seen that the scatter of the data is further reduced when stagnation pressure ratio is used for the plot of results instead of static pressure ratio. The static pressure ratio is a readily available quantity in a compressor test. But stagnation pressure combines the pressure and kinetic energy to a quantity that is a measure of total energy content in the fluid stream. Therefore, the ratio of stagnation pressure provides a measure of energy increase as the fluid passes through the compressor impeller. In Figure 4, it can also be noticed that for different valve openings the data show a nice monotonic increase of stagnation pressure ratio with blade Mach number.

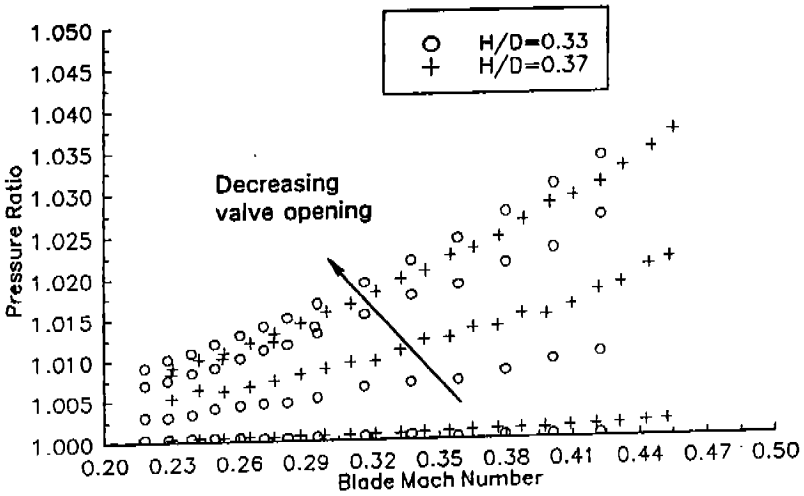


Figure 3. Pressure Ratio for Small Centrifugal Compressors

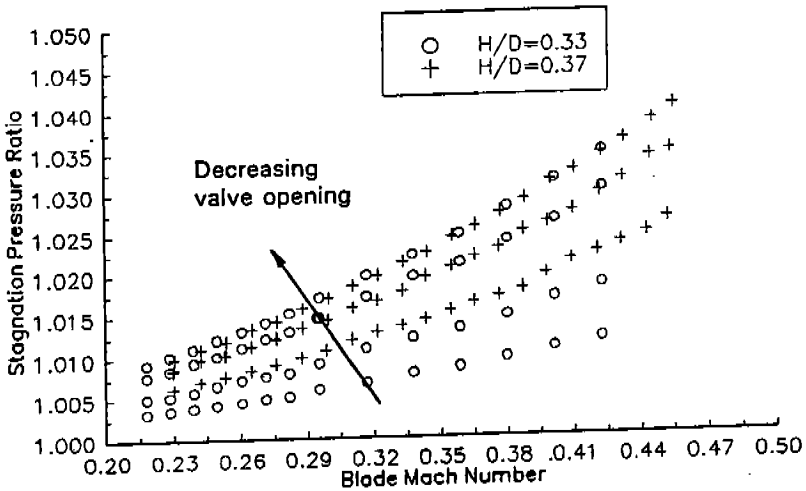


Figure 4. Distribution of Stagnation Pressure Ratio

The variation of stagnation temperature ratio with blade Mach number is shown in Figure 5. For a given Mach number, a larger rise in stagnation temperature is seen in most experimental runs for a larger H/D ratio. The stagnation temperature also rises with blade Mach number since more work is input to the system. The distribution of Reynolds number with flow coefficient is presented in Figure 6. The Reynolds number increases with flow coefficient monotonically, and all experimental data fall into a single curve. This curve can be used for any general prediction of Reynolds number which determines the flow regime in impeller blade passages.

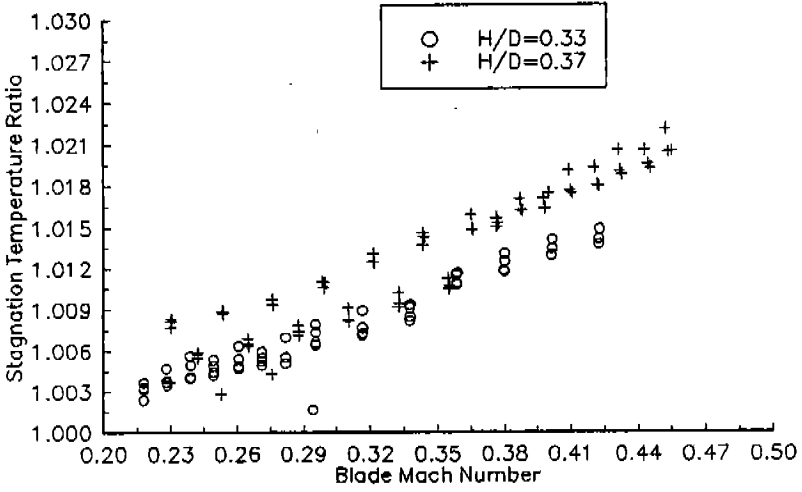


Figure 5. Distribution of Stagnation Temperature Ratio

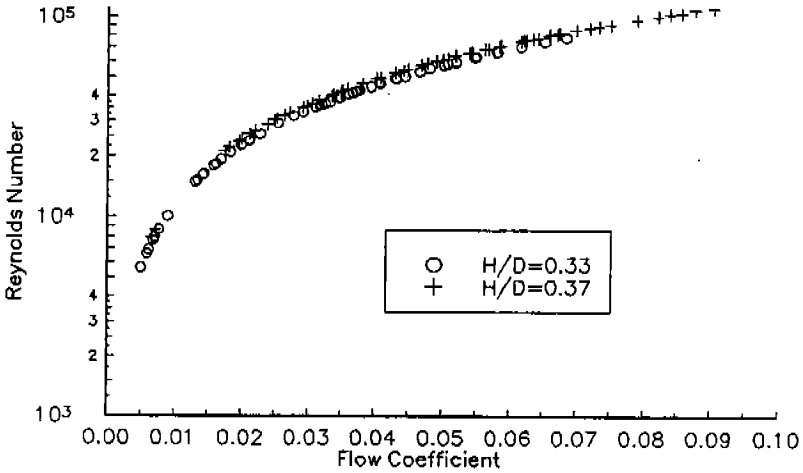
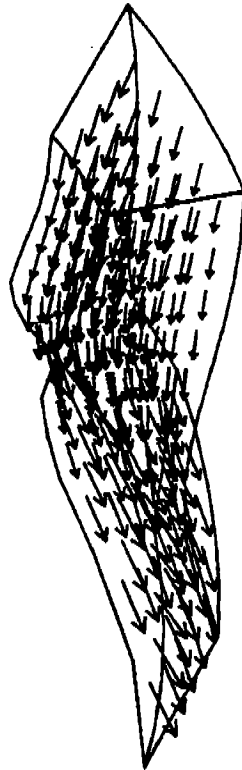


Figure 6. Reynolds Number for Small Centrifugal Compressors

NUMERICAL COMPUTATIONS

A detailed computation of flow in impeller blade passages was done to understand the fluid flow characteristics in the compressor impellers. The blade profile of one of the impellers ($D=2.365$ inch, $H/D=0.73$) that was used for the experiment was measured and was provided as input to generate the boundary of the computation domain. A non-orthogonal, boundary-fitted grid structure was generated from these boundary points to cover one single flow passage between two impeller blades. Even though the grid structure was generated from a reference Cartesian coordinate frame, the computation was performed using a curvilinear coordinate frame attached to the flow. The equations for the conservation of mass and momentum were solved in their complete three-dimensional form to generate the values of velocity components and pressure distribution in the flow field. The discretization of these equations was made using a control-volume approach [6] where these equations were integrated locally for each grid cell, taking into account the appropriate amount of convection and diffusion from the neighboring



→ : 100.0 m/s.

Figure 7. Velocity Vectors in a Radial Flow Compressor Impeller
(RPM=6000, $D=2.365$ inch, $H=0.773$ inch)

cells. The storage of different quantities in a grid cell was done in a staggered fashion, where pressure was stored at the center and velocity components at cell boundaries. The equations were solved using SIMPLEST algorithm [7], which used an iterative solution procedure that updates velocity and pressure by solving the momentum and mass conservation equations, respectively. The convergence was monitored by looking at the field values at selected locations and the sum of residuals for each conservation equation for the entire computation domain. Computations were continued until spot checked field values reached an invariant condition up to the fourth place of decimal and sum of the residuals reached below 10^{-7} .

The plot of the velocity vectors for two different rotational speeds are shown in Figures 7 and 8, respectively. It can be seen that the velocity increases substantially with rotational speed since more kinetic energy of the impeller is transferred to the fluid. For any given rotational speed, the fluid velocity also increases as it passes through the impeller blade passage. This is because of the transfer of the rotational kinetic energy from impeller to the fluid as it passes through the impeller. The transfer of fluid kinetic energy to pressure is done in the diffuser of the compressor which follows the impeller. The flow pattern seen here is fairly well structured, which is expected at small values of Reynolds and Mach numbers.

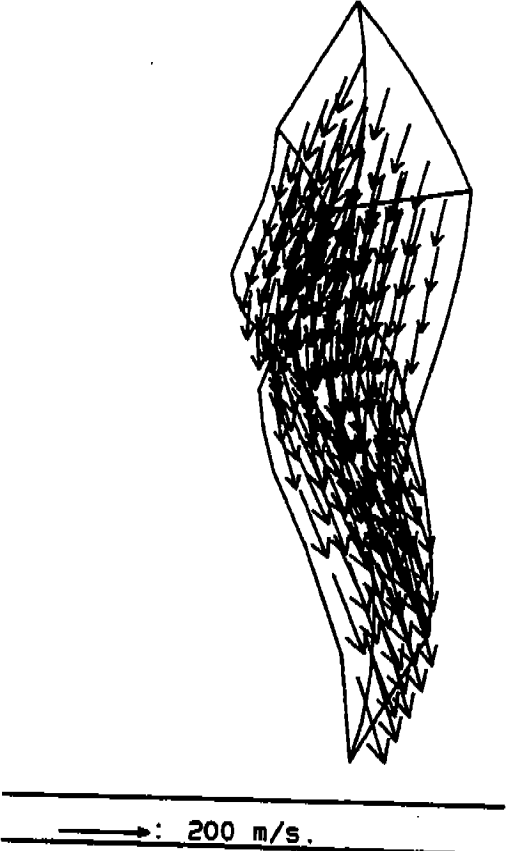


**Figure 8. Velocity Vectors in a Radial Flow Compressor Impeller
(RPM=18000, D=2.365 inch, H=0.773 inch)**

CONCLUSIONS

Experimental measurements and numerical computations were performed to determine the characteristics of small centrifugal compressors for possible applications in air-cycle power and refrigeration systems. Tests were performed for different rotational speeds and flow rates. The data were used to calculate the important dimensionless parameters which were independently determined from a fundamental dimensional analysis. The results showed that for a given flow coefficient, the ratio of stagnation pressures increases monotonically with blade Mach number. For a given rotational speed, the stagnation pressure ratio decreased with flow coefficient. It was also found that the Reynolds number increases monotonically with flow coefficient and all experimental data lined into a single curve that can be used for general prediction. The fluid velocity inside impeller passages were found to be well structured at small flow rates and rotational speeds. The magnitude of the velocity increased with rotational speed because of the larger transfer of kinetic energy from the impeller to the fluid stream.

ACKNOWLEDGMENTS

Funding for this research was obtained from U.S. Army R D & E Center in Natick, MA under contract number DAAK60-91-C-0061 and from U.S. Army Tank Automotive Command, Warren, MI under contract number DAAE07-91-C-R020.

REFERENCES

1. Rahman, M.M. and Scaringe, R.P., "Development of an Air-Cycle Micro-Climate Cooling Device," Phase I Final Report, U.S. Army R D & E Center, Natick, MA, Mainstream Engineering Corporation Report, April, 1992.
2. Rahman, M.M., Parrish, C.F., and Scaringe, R.P., "Innovative TACOM Personnel Heater," Phase I Final Report, U.S. Army Tank Automotive Command, Warren, MI, Mainstream Engineering Corporation Report, January, 1992.
3. Van Wylen, G.J. and Sonntag, R.E., Fundamentals of Classical Thermodynamics, Second Edition, John Wiley and Sons, N.Y., 1978.
4. Dixon, S.L., Fluid Mechanics, Thermodynamics of Turbomachinery, Third Edition, Pergamon Press, Oxford, 1978.
5. Taylor, E.S., Dimensional Analysis for Engineers, Clarendon Press, Oxford, 1974.
6. Patankar, S.V., Numerical Heat Transfer and Fluid Flow, Hemisphere Publishing Corporation, N.Y., 1980.
7. Spalding, D.B., "Mathematical Modeling of Fluid Mechanics, Heat Transfer and Chemical Reaction Processes," A Lecture Course, CFDU HTS/80/1, Imperial College, London, U.K., 1980.